NASA TECHNICAL NOTE

NASA TN D-4124

NASA TN D-4124

BUCKLING OF A PRESSURIZED TOROIDAL RING UNDER UNIFORM EXTERNAL LOADING

by George E. Weeks

Langley Research Center

Langley Station, Hampton, Va.

NATIONAL AERONAUTICS AND SPACE ADMINISTRATION • WASHINGTON, D. C. • AUGUST 1967

BUCKLING OF A PRESSURIZED TOROIDAL RING UNDER UNIFORM EXTERNAL LOADING

By George E. Weeks
Langley Research Center

SUMMARY

A theoretical investigation of the buckling of a pressurized toroidal ring under a uniformly distributed line load is carried out, with finite shear stiffness, extensional stiffness, and appropriate contributions from the internal pressure taken into account. The equations governing both in-plane and out-of-plane buckling behavior of the ring, with direction of loading included, are derived and solved. The solutions to the buckling equations are presented in terms of five general parameters which are functions of the internal pressure, external load, and ring geometry.

The major results of the investigation are: (a) The magnitude of the buckling load is very sensitive to the direction of loading during the buckling deformation and to the ratio of cross-sectional radius to the radius of the ring; (b) the shear stiffness of the ring wall material and internal pressure both contribute to the effective transverse shear stiffness of the ring, which strongly influences the buckling loads.

INTRODUCTION

Expandable structures capable of being packaged into a small volume and erected into load-carrying structures by inflation have been used for a number of space missions. One such structure is an inflatable toroidal ring which has potential use as a stiffening element of deployable aerospace structures; for example, it may be efficient as a stiffening ring of a deployable planetary entry decelerator.

To use this ring in a practical structure, its buckling strength under compressive loads must be determined. Investigations of the stability of rings under uniform loads may be found in references 1, 2, and 3. These studies, however, do not account for finite transverse shear stiffness including effects of internal pressure, which can be expected to be important for inflatable rings.

The purpose of the present paper is to determine the buckling load of a pressurized toroidal ring subjected to a uniformly distributed radial load, taking transverse shear deformation into account. Since the investigations of references 1 to 3 have shown that

the direction of load during deformation can have a significant effect on the magnitude of the resulting buckling load, three directions of load during the buckling process are considered: (a) The load remains in the same direction, (b) the load remains directed toward the initial center of curvature, (c) the load remains normal to the deformed surface at every point. Both in-plane and out-of-plane ring behavior are included.

SYMBOLS

$A = 2\pi rt$

$\overline{A} = \pi r^2$

A^* cross-sectional area of toroidal membrane perpendicular to the centroidal axis after deformation (see fig. 3)

$c = \frac{r}{R}$

e_α local circumferential extensional strain in membrane

$e_{\alpha\theta}$ local shear strain in membrane

E Young's modulus

G shear modulus

I area moment of inertia of membrane

J area polar moment of inertia of membrane

$K, \overline{K}$ determinants defined by equations (44a) and (50a), respectively

M_1 twisting moment about the centroidal axis (see fig. 1)

n integer

$N_{\alpha\theta}$ local shear-stress resultant

p internal pressure

P internal-pressure stiffness parameter, $p\overline{A}R^2/EI$

q	external uniform line load
$\bar{q}$	external load parameter, qR^3/EI
$Q, \bar{Q}$	determinants defined by equations (44c), (44d), (44e), (50c), and (50d)
r	radius of cross section of toroidal membrane
R	radius from origin to centroidal axis of toroidal membrane
$\bar{R}$	radius parameter defined by equation (11)
$\bar{\bar{R}}$	radius parameter defined by equation (36)
s^*	length of centroidal axis after deformation
$\bar{s}^*$	length of outer surface of deformed ring in contact with line load
S	shear-stiffness parameter, $AGR^2/2EI$
t	membrane wall thickness
T	extensional-stiffness parameter, EAR^2/EI
u_1, u_2, u_3	tangential, radial, and out-of-plane rigid-body translations of cross section of ring
u, v, w	tangential and normal displacements of a point in the surface of the membrane (see fig. 1)
V_2, V_3	shear forces in the y and z directions, respectively (see fig. 1)
W	work of external load
x, y, z	rectangular Cartesian coordinates (see fig. 1)
$Z, \bar{Z}$	determinants defined by equations (44b) and (50b), respectively
α	circumferential angular coordinate of centroidal axis

β angle defined by equation (14) (see fig. 2)

$\bar{\beta}$ angle defined by equation (37) (see fig. 7)

γ_2, γ_3 shear strain of cross section in y and z directions, respectively

Γ twisting-stiffness parameter, JG/EI

$\Delta\bar{R}$ radial distance of point on deformed outer surface from corresponding point on undeformed outer surface, under the line load

ΔV change in enclosed volume of membrane due to deformation

$\Delta\Omega$ net area enclosed by deformed and undeformed membrane at its outer surface

θ angular coordinate of ring cross section

Π_1 change in strain energy of deformed membrane

Π_2 change in potential energy of internal pressure

Π_3 additional energy of the shell due to buckling

$\omega_1, \omega_2, \omega_3$ rotation of ring cross section in yz, xz, and xy planes, respectively

Subscripts:

a constant-direction loading

b radial loading

c hydrostatic loading

cr critical

ANALYSIS

A segment of a pressurized toroidal ring configuration and the coordinate systems are shown in figure 1. The radius of the ring is R and the radius of the cross section is r. The angular coordinates α and θ are in the plane of the ring and in the plane

of the ring cross section, respectively. They thus define the position of a point on the surface of the ring. Displacements u, v, and w of points on the surface of the ring are related to rigid-body translations of and rotations about the centroidal axis of the ring. Translations u_i of the centroidal axis are referred to a local Cartesian coordinate system with its origin along the centroidal axis: u_1 is tangential to the centroidal axis; u_2 and u_3 lie in the plane of the ring cross section. Rigid-body rotations ω_i are referred to this same local coordinate system. These directions are shown in figure 2.

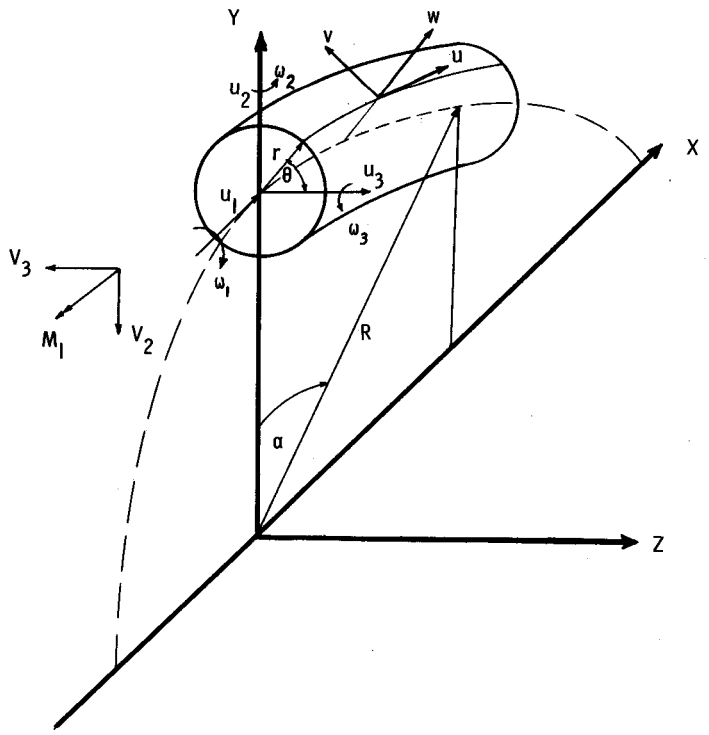

Figure 1.- Ring-segment configuration and coordinate systems.

Certain simplifying assumptions have been made in this analysis: (1) The ring is considered to be a membrane in that the local bending stiffness of the shell walls is neglected, (2) the ring buckles without localized wrinkling of the membrane walls, (3) any cross section of the ring remains rigid in its own plane so that the cross section remains circular and the resulting deformations can be characterized by the six rigid-body motions of translation and rotation of the cross section, (4) the rigid-body rotations are small enough for the displacements on the surface of the toroidal ring to be represented by the vector sums of the displacements due to translations and rotations of a cross section.

Derivation of Governing Equations

The buckling equations of the pressurized toroidal ring deforming about some prestressed equilibrium configuration can be obtained from the variational equation

$$\delta\Pi_1 + \delta\Pi_2 + \delta\Pi_3 - \delta W = 0 \tag{1}$$

where Π_1 is the change in strain energy, Π_2 is the potential-energy change of the internal pressure, Π_3 is the potential energy of the prebuckling membrane stress acting through the buckling strain, and W is the work done by the externally applied loads during buckling.

Local buckling displacements in terms of rigid-body motions of a cross section.- The local displacements u, v, and w of a circular toroidal ring can be expressed in terms of the rigid-body motions u_i and ω_i of a cross section. These are identical to those given in reference 4 for a circular cylindrical beam. They are

$$u = u_1 + r\omega_2 \cos\theta - r\omega_3 \sin\theta \tag{2a}$$

$$v = -r\omega_1 + u_2 \cos\theta - u_3 \sin\theta + \frac{r}{2}\left(\omega_2^2 - \omega_3^2\right)\sin\theta \cos\theta \tag{2b}$$

$$w = u_2 \sin\theta + u_3 \cos\theta - \frac{r}{2}\left(\omega_1^2 + \omega_2^2\cos^2\theta + \omega_3^2\sin^2\theta\right) \tag{2c}$$

Note that u_i and ω_i are functions of α only.

Strain energy of the toroidal ring.- If it is assumed that the strain e_θ in the θ direction is negligible, the strain energy Π_1 for the toroidal membrane ring becomes

$$\Pi_1 = \frac{t}{2}\int_0^{2\pi}\int_0^{2\pi}\left(Ee_\alpha^2 + Ge_{\alpha\theta}^2\right)(R + r\sin\theta)r\, d\alpha\, d\theta \tag{3}$$

The strain displacement relations for a toroidal membrane are (ref. 5), after some manipulation,

$$e_\alpha = \frac{u_{,\alpha} + v\cos\theta + w\sin\theta}{R + r\sin\theta} + \frac{1}{2(R + r\sin\theta)^2}\left(v_{,\alpha}^2 + w_{,\alpha}^2 + u^2 - 2uw_{,\alpha}\sin\theta - 2uv_{,\alpha}\cos\theta\right) \tag{4}$$

$$e_{\alpha\theta} = \frac{u_{,\theta}}{r} + \frac{v_{,\alpha} - u\cos\theta}{R + r\sin\theta} \tag{5}$$

where commas denote differentiation with respect to the subscripts. Nonlinear terms are retained in e_α in order to take into account the nonlinear stretching of the ring during buckling. However, for the theory considered here, it is adequate to include only the linear terms in the shear-strain displacement relation.

These strains can be expressed in terms of the rigid-body rotations and translations of a cross section of the ring by substituting equations (2) into equations (4) and (5). The results are

$$e_\alpha = \frac{1}{R + r\sin\theta}\left[u_1' + u_2 + r\cos\theta(\omega_2' - \omega_1) - r\sin\theta\left(\omega_3' + \frac{\omega_3^2}{2} + \frac{\omega_1^2}{2}\right)\right]$$

$$+ \frac{1}{2(R + r\sin\theta)^2}\left[r^2(\omega_1')^2 + (u_3')^2 + u_1^2 + u_2'(u_2' - 2u_1)\right.$$

$$+ 2r\sin\theta(\omega_1'u_3' + \omega_3u_2' - \omega_3u_1) - 2r\cos\theta(u_2' - u_1)(\omega_1' + \omega_2)$$

$$\left. + r^2\omega_3^2\sin^2\theta + r^2\omega_2\cos^2\theta(\omega_2 + 2\omega_1') - 2r^2\omega_3\sin\theta\cos\theta(\omega_2 + \omega_1')\right] \qquad (6a)$$

$$e_{\alpha\theta} = \frac{1}{R + r\sin\theta}\left[-r\omega_1' - (R + r\sin\theta)(\omega_2\sin\theta + \omega_3\cos\theta)\right.$$

$$\left. + \sin\theta(-u_3') + \cos\theta(u_2' - u_1) - r\omega_2\cos^2\theta + r\sin\theta\cos\theta(\omega_3)\right] \qquad (6b)$$

where primes denote differentiation with respect to α. If equations (6) are substituted into equation (3) and the result is integrated over θ, the variation of the strain energy Π_1 becomes (retaining all terms up to order $(r/R)^2$):

$$\delta\Pi_1 = \frac{\delta}{2}\int_0^{2\pi}\left[\left(EA + \frac{EI}{R^2}\right)\left(\frac{u_1' + u_2}{R}\right)^2 + EI\left(\frac{\omega_2' - \omega_1}{R}\right)^2 + EI\left(\frac{\omega_3'}{R}\right)^2 + \frac{2EI}{R^2}\omega_3'\left(\frac{u_1' + u_2}{R}\right)\right.$$

$$+\left(\frac{GA}{2} + \frac{3}{8}\frac{GJ}{R^2}\right)\left(\omega_2 + \frac{u_3'}{R}\right)^2 + \left(\frac{GA}{2} + \frac{GJ}{8R^2}\right)\left(\omega_3 - \frac{u_2' - u_1}{R}\right)^2 + GJ\left(\frac{\omega_1' + \omega_2}{R}\right)^2$$

$$\left. - \frac{GJ}{R^2}(\omega_1' + \omega_2)\left(\frac{\omega_2 + u_3'}{R}\right)\right]R\,d\alpha \qquad (7)$$

where

$$I = \pi r^3 t \qquad J = 2\pi r^3 t \qquad A = 2\pi r t$$

It should be noted that the equations here are applicable to an orthotropic material since e_θ was assumed to be zero. Therefore, to define the stiffness characteristics of the ring, it was only necessary to define the four effective stiffness quantities EA, EI, GA, and GJ.

Potential energy of the pressurizing gas.- The work done by the internal pressure is the product of the pressure and the change in enclosed volume due to deformation. The internal pressure is assumed to remain constant during buckling. Since the cross section of the ring is assumed to remain circular and to move as a rigid body during deformation, the change in volume is

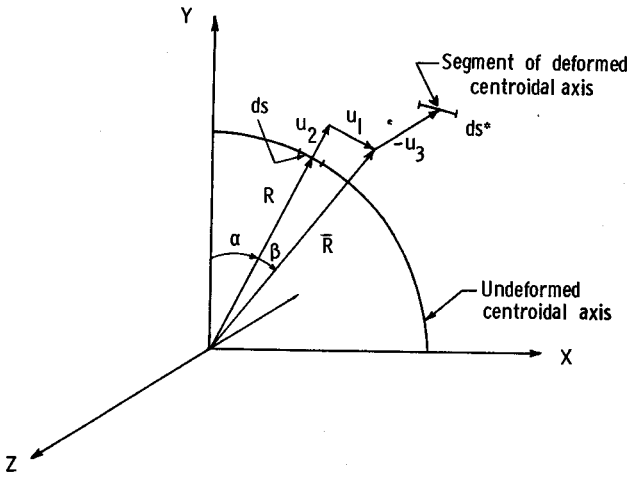

Figure 2.- Geometry of deformation of centroidal axis of ring.

$$\Delta V = \int_{s^*} A^* ds^* - 2\pi R\bar{A} \tag{8}$$

where ds^* is a differential length along the centroidal axis of the ring after buckling (see fig. 2), A^* is the area normal to the deformed centroidal axis, and $\bar{A} = \pi r^2$.

The radial, tangential, and out-of-plane displacements of the centroidal axis of the ring in terms of the rigid-body displacements are u_2, u_1, and $-u_3$, respectively.

The length ds^* can be expressed in the fundamental form

$$(ds^*)^2 = dx^2 + dy^2 + dz^2 \tag{9}$$

where

$$\left.\begin{aligned} x &= \bar{R}\sin(\alpha + \beta) \\ y &= \bar{R}\cos(\alpha + \beta) \\ z &= -u_3 \end{aligned}\right\} \tag{10}$$

and

$$\bar{R} = \sqrt{(R + u_2)^2 + u_1^2} \tag{11}$$

Substituting equations (10) and (11) into equation (9) gives

$$(ds^*)^2 = \left[1 + 2\beta' + (\beta')^2\right]\bar{R}^2 d\alpha^2 + (d\bar{R})^2 + (du_3)^2$$

which can be written as

$$(ds^*)^2 = \left[1 + 2\beta' + (\beta')^2 + \frac{(\bar{R}')^2}{\bar{R}^2} + \frac{(u_3')^2}{\bar{R}^2}\right]\bar{R}^2 d\alpha^2 \tag{12}$$

where

$$\overline{R} = R\left(1 + \frac{u_2}{R} + \frac{u_1^2}{2R^2} + \ldots\right) \tag{13}$$

$$\beta = \tan^{-1}\frac{u_1}{R + u_2} = \frac{u_1}{R + u_2} + \ldots \tag{14}$$

Expanding equation (12) and retaining up to second-order terms in the displacements gives

$$ds^* = \left\{1 + \frac{u_1' + u_2}{R} + \frac{1}{2R^2}\left[u_1^2 + (u_2')^2 + (u_3')^2 - 2u_1u_2'\right]\right\} R\, d\alpha \tag{15}$$

To obtain the area A^* normal to the deformed centroidal axis, note that the cross-sectional area $\overline{A}$ is unchanged but is no longer perpendicular to the deformed axis at coordinates $(\overline{R}, \alpha+\beta, -u_3)$ because of the shear deformations of the ring. An illustration of this effect for only the shear deformation in the plane of the ring γ_2 is shown in figure 3.

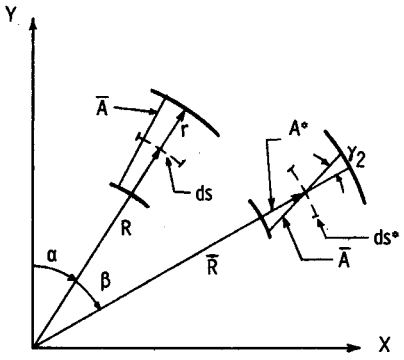

Figure 3.- Cross-sectional area $\overline{A}$ before and after shear deformation γ_2 of the ring.

From figure 3, the area A^* can be expressed in terms of the original area $\overline{A}$ by the equation $A^* = \overline{A}\cos\gamma_2$, or taking into account shear deformation both in the plane and perpendicular to the plane of the ring leads to

$$A^* = \overline{A}\cos\gamma_2\cos\gamma_3 \tag{16}$$

If the shear strains γ_2 and γ_3 are small,

$$A^* = \overline{A}\left(1 - \frac{\gamma_2^2}{2} - \frac{\gamma_3^2}{2}\right) \tag{17}$$

With γ_2 and γ_3 known, equations (15) and (17) can be substituted into equation (8) to obtain the change in volume.

An expression for γ_2 and γ_3 can be found in the following manner: The local shear-stress resultant $N_{\alpha\theta}$ can be expressed in terms of ring shear and moment resultants as

$$N_{\alpha\theta} = -\frac{M_1}{2\pi r^2} + \frac{V_2\cos\theta}{\pi r} - \frac{V_3\sin\theta}{\pi r} \tag{18}$$

where M_1 is the twisting moment and V_2 and V_3 are the shear forces in the plane of the ring cross section. (See fig. 1.) The energy due to shear can be written as

$$U_S = \frac{1}{2}\int_0^{2\pi}\int_0^{2\pi} N_{\alpha\theta} e_{\alpha\theta} R(1 + r \sin\theta) r \, d\alpha \, d\theta \tag{19}$$

Substituting equations (6b) and (18) into equation (19) and integrating over θ yields the following result:

$$U_S = \frac{1}{2}\int_0^{2\pi}\left[M_1 \frac{\omega_1' + \omega_2}{R} + V_2\left(-\omega_3 + \frac{u_2' - u_1}{R}\right) + V_3\left(\omega_2 + \frac{u_3'}{R}\right)\right] R \, d\alpha \tag{20}$$

The coefficients of V_2 and V_3 are the desired quantities γ_2 and γ_3, respectively. Hence

$$\left.\begin{aligned} \gamma_2 &= -\omega_3 + \frac{u_2' - u_1}{R} \\ \gamma_3 &= \omega_2 + \frac{u_3'}{R} \end{aligned}\right\} \tag{21}$$

Substituting equations (15) and (17) into (8), using equations (21), and retaining up to quadratic terms in the displacements gives the change in volume of the ring due to deformation as

$$\Delta V = \int_0^{2\pi} \overline{A}\left(\frac{u_1' + u_2}{R} + \frac{\omega_3 u_2' - \omega_3 u_1 - u_3'\omega_2}{R} - \frac{\omega_2^2 + \omega_3^2}{2}\right) \tag{22}$$

With $\Pi_2 = -p\,\Delta V$, the variation in the potential energy resulting from internal pressure can be written as

$$\delta\Pi_2 = -p\overline{A}\,\delta\int_0^{2\pi}\left(\frac{u_1' + u_2}{R} + \frac{\omega_3 u_2' - \omega_3 u_1 - u_3'\omega_2}{R} - \frac{\omega_2^2 + \omega_3^2}{2}\right) R \, d\alpha \tag{23}$$

Additional potential energy of prebuckling membrane stress.- In order to take into account buckling behavior, the change in potential energy of the prebuckling membrane stresses due to a uniform line load q, as they act through the nonlinear buckling displacements, must be accounted for. The prebuckling membrane stress is taken to be

$$\sigma_o = \frac{-qR(1 + c) + p\overline{A}}{A} \tag{24}$$

This membrane stress acts through the strain given by equation (6a). Hence the variation of this energy while it acts through the buckling displacements is given by

$$\delta\Pi_3 = \delta\int_0^{2\pi}\int_0^{2\pi} \sigma_o e_\alpha rt(R + r \sin\theta) d\theta \, d\alpha \tag{25}$$

Substituting equation (6a) into equation (25), integrating, and retaining terms up to order c^2 results in

$$\delta\Pi_3 = \frac{-qR(1 + c) + p\overline{A}}{2}\,\delta\int_0^{2\pi}\left[2\,\frac{u_1' + u_2}{R} + \frac{(u_3')^2 + u_1^2}{R^2} + \frac{u_2'(u_2' - 2u_1)}{R^2}\right]R\,d\alpha \qquad (26)$$

Work done by the external loads.- The toroidal ring is loaded by a uniformly distributed radial line load q acting on the outer surface of the cross section. (See fig. 4.) The load q is initially directed toward the center, but during buckling it is assumed to behave in one of the following ways: (a) The load remains in the same direction (constant-direction loading), (b) the load remains directed toward the center of initial curvature (radial loading), and (c) the load remains normal to the deformed surface at every point (hydrostatic loading).

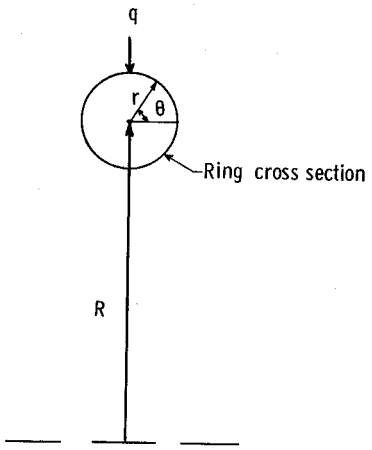

Figure 4.- Direction of external line load q.

To evaluate the work done by three loading conditions, it is necessary to express the local displacements of a point on the surface of the shell directly under the line load in terms of the rigid-body motions of the cross section of the ring. Since $\theta = \pi/2$ directly under the line load (see fig. 4), the local displacements at the point of the load can be obtained from equations (2) as

$$\left.\begin{aligned} u_{\theta=\pi/2} &= u_1 - r\omega_3 \\ v_{\theta=\pi/2} &= -r\omega_1 - u_3 \\ w_{\theta=\pi/2} &= u_2 - \frac{r}{2}\left(\omega_1^2 + \omega_3^2\right) \end{aligned}\right\} \qquad (27)$$

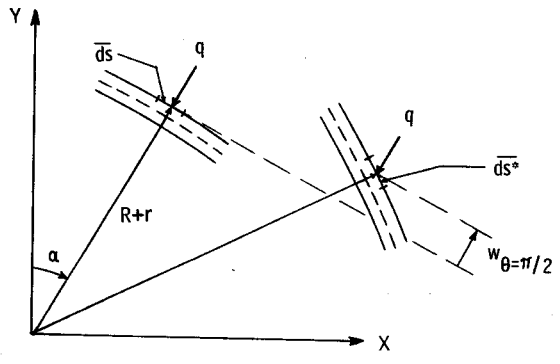

Figure 5.- Geometry of constant-direction loading.

(a) For the constant-direction loading (see fig. 5) the variation in the external work is

$$\delta W_a = -\int_{s^*} q\,\overline{ds}^*\,\delta w_{\theta=\pi/2} \qquad (28)$$

where $\overline{ds}^*$ is an infinitesimal length of the outer surface of the ring directly under the external load q. This infinitesimal length $\overline{ds}^*$ is obtained from equations (9), (10), and (11) by using the displacements u, v, and w

from equations (27) in place of u_1, $-u_3$, and u_2, respectively. The result is (keeping up to first-order terms in displacements)

$$\overline{ds}^* = \left(1 + \frac{u_1' - Rc\omega_3' + u_2}{R(1 + c)}\right)R(1 + c)d\alpha \tag{29}$$

and the variation in the external work becomes

$$\delta W_\alpha = -qR(1 + c)\int_0^{2\pi}\left\{\left[1 + \frac{u_1' - Rc\omega_3' + u_2}{R(1 + c)}\right]\delta\left(\frac{u_2}{R} - \frac{c\omega_1^2}{2} - \frac{c}{2}\omega_3^2\right)\right\}R\,d\alpha \tag{30}$$

(b) For radial loading (fig. 6) the variation in the external work is

$$\delta W_b = -\int_{s^*} q\,\overline{ds}^*\,\delta\Delta\overline{R} \tag{31}$$

where $\overline{ds}^*$ is given by equation (29) and $\Delta\overline{R}$ is the radial distance of a point on the outer surface of the deformed ring from the corresponding point on the undeformed outer surface.

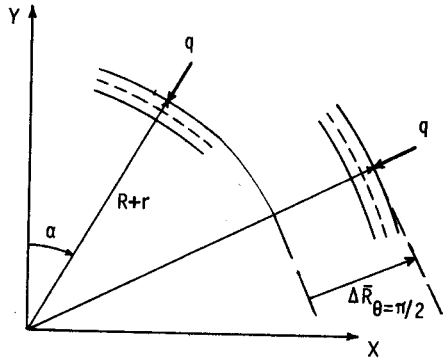

Figure 6.- Two-dimensional representation for geometry of radial loading.

Retaining up to quadratic terms in the displacements gives

$$\Delta\overline{R} = \left[w + \frac{u^2}{2(R + r)} + \frac{v^2}{2(R + r)}\right]_{\theta=\pi/2} \tag{32}$$

Substituting this expression for $\Delta\overline{R}$ into equation (31) and making use of equations (27) and (29) leads to the following equation for the external virtual work:

$$\delta W_b = -qR(1 + c)\int_0^{2\pi}\left[1 + \frac{u_1' - Rc\omega_3 + u_2}{R(1 + c)}\right]\delta\left\{\frac{u_2}{R} - \frac{c}{2}\left(\omega_1^2 + \omega_3^2\right)\right.$$

$$\left. + \frac{1 - c + c^2 \ldots}{2}\left[\frac{u_1^2 + u_3^2}{R^2} - \frac{2c}{R}\left(u_1\omega_3 - u_3\omega_1\right) + c^2\left(\omega_3^2 + \omega_1^2\right)\right]\right\}R\,d\alpha \tag{33}$$

(c) For the hydrostatic loading, the variation in the external work is

$$\delta W_c = -q\,\delta\Delta\Omega \tag{34}$$

where $\Delta\Omega$ is the net area enclosed by the deformed and undeformed ring surface at its outer extremity. (See fig. 7. Here, the area enclosed by the undeformed ring surface at

its outer extremity is $\pi(R + r)^2$.) For simplicity the out-of-plane contribution to this work term will not be considered, so that it is only necessary to consider the two-dimensional deformations shown in figure 7. Hence, the resulting buckling loads for the hydrostatic loading will be applicable only for in-plane behavior. From figure 7 is seen that $\Delta\Omega$ can be represented by the equation

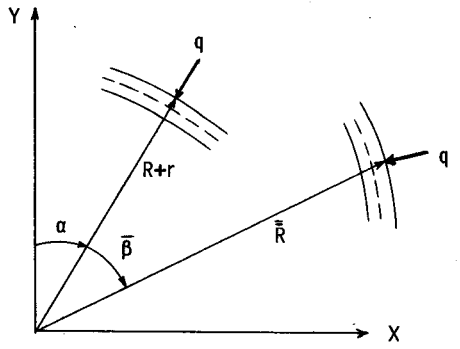

Figure 7.- Two-dimensional representations for geometry of hydrostatic loading. Displacements are evaluated at $\theta = \pi/2$.

$$\Delta\Omega = \frac{1}{2}\int_0^{2\pi}\left[\bar{\bar{R}}^2\left(1 + \frac{d\bar{\beta}}{d\alpha}\right)\right]d\alpha \tag{35}$$

where

$$\bar{\bar{R}} = (R + r)\left[1 + \frac{w}{R + r} + \frac{u^2}{2(R + r)^2}\right]_{\theta=\pi/2} \tag{36}$$

and

$$\bar{\beta} = \left(\frac{u}{R + r + w}\right)_{\theta=\pi/2} \tag{37}$$

Substitution of equations (36) and (37) into equation (35) results in

$$\Delta\Omega = \frac{1}{2}(R + r)^2\int_0^{2\pi}\left[\frac{1}{R + r}(u' + 2w) + \frac{1}{(R + r)^2}\left(u^2 + w^2 + u'w - uw'\right)\right]_{\theta=\pi/2} d\alpha \tag{38}$$

After substitution of equation (38) into equation (34) and making use of equations (27), the variation in the work of the hydrostatic line load q is

$$\delta W_c = -qR(1 + c)\delta\int_0^{2\pi}\frac{1}{2}\left[\left(\frac{u_1' + 2u_2}{R} - c\omega_3' - c\omega_1^2 - c\omega_3^2\right) + \frac{1 - c + c^2 \cdot \cdot \cdot}{R^2}\left(u_1^2 + u_2^2\right.\right.$$

$$\left.\left. + R^2c^2\omega_3^2 - 2Rcu_1\omega_3 + u_1'u_2 - u_1u_2' - Rcu_2\omega_3' + Rcu_2'\omega_3\right)\right]R\, d\alpha \tag{39}$$

Buckling equations.- The buckling equations are now obtained by substituting equations (7), (23), (26), (30), (33), and (39) into equation (1), taking the indicated variation, and integrating by parts where necessary. Equating the coefficients of the arbitrary variations δu_1, δu_2, $\delta\omega_3$, $\delta\omega_1$, $\delta\omega_2$, and δu_3 separately to zero yields

$$-(T + 1)\left(u_1'' + u_2'\right) + (P + S)\left(R\omega_3 + u_1 - u_2'\right) - R\omega_3'' - \bar{q}(1 + c)\left(u_1 - u_2'\right)$$

$$+ \underline{\bar{q}\left(u_1 - cR\omega_3\right)} + \underline{\underline{\bar{q}\left(u_1 - u_2' - cR\omega_3\right)}} = 0 \tag{40a}$$

$$(T + 1)(u_1' + u_2) + (P + S)(R\omega_3' + u_1' - u_2'') + R\omega_3' - \bar{q}(1 + c)(u_1' - u_2'')$$

$$+ \underline{\bar{q}(u_1' + u_2 - cR\omega_3')} + \underline{\underline{\bar{q}(u_1' + u_2 - cR\omega_3')}} + \underline{\underline{\underline{\bar{q}(u_1' - cR\omega_3' + u_2)}}} = 0 \qquad (40b)$$

$$-R\omega_3'' - (u_1'' + u_2') - (P + S)(-R\omega_3 - u_1 + u_2') - \underline{\bar{q}cR\omega_3} - \underline{\underline{\bar{q}c(u_1 + R\omega_3)}}$$

$$+ \underline{\underline{\underline{\bar{q}c(-R\omega_3 - u_1 + u_2')}}} = 0 \qquad (40c)$$

$$-R(\omega_2' - \omega_1) - R\Gamma\left(\omega_1'' + \frac{\omega_2'}{2} - \frac{u_3''}{2R}\right) - \underline{\bar{q}cR\omega_1} - \underline{\underline{\bar{q}c(-u_3 + R\omega_1)}} - \underline{\underline{\bar{q}cR\omega_1}} = 0 \qquad (40d)$$

$$-R(\omega_2'' - \omega_1') + \left(P + S + \frac{3}{8}\Gamma\right)(u_3' + R\omega_2) + R\Gamma\left(\frac{\omega_1'}{2} - \frac{u_3'}{2R}\right) = 0 \qquad (40e)$$

$$-\left(P + S + \frac{3}{8}\Gamma\right)(u_3'' + R\omega_2') + \frac{R\Gamma}{2}(\omega_1'' + \omega_2') + \bar{q}(1 + c)u_3'' + \underline{\underline{\bar{q}(u_3 + Rc\omega_1)}} = 0 \qquad (40f)$$

where

$$\bar{q} = \frac{qR^3}{EI} \qquad S = \frac{AGR^2}{2EI} \qquad P = \frac{p\bar{A}R^2}{EI} \qquad T = \frac{EAR^2}{EI} \qquad \Gamma = \frac{JG}{EI} \qquad (41)$$

The single-underlined terms in equations (40) apply for a constant-direction load (case a), the double-underlined terms for a radial load (case b), and the triple-underlined terms for a hydrostatic load (case c). Note that the in-plane buckling behavior is not coupled with out-of-plane buckling. The first three equations, (40a), (40b), and (40c), describe in-plane buckling in terms of the in-plane variables u_1, u_2, and ω_3. The second three equations, (40d), (40e), and (40f), describe out-of-plane buckling in terms of the variables u_3, ω_1, and ω_2.

Solutions of the Buckling Equations

A solution to equations (40) may be taken in the form

$$u_1 = \bar{u}_1 \sin n\alpha \qquad (42a)$$

$$u_2 = \bar{u}_2 \cos n\alpha \qquad (42b)$$

$$\omega_3 = \bar{\omega}_3 \sin n\alpha \qquad (42c)$$

$$\omega_1 = \bar{\omega}_1 \sin n\alpha \qquad (42d)$$

$$\omega_2 = \bar{\omega}_2 \cos n\alpha \tag{42e}$$

$$u_3 = \bar{u}_3 \sin n\alpha \tag{42f}$$

where n represents the number of buckle waves and $\bar{u}_i$ and $\bar{\omega}_i$ are constants.

In-plane buckling.- The solution for the in-plane buckling for each of the three loading conditions cited previously is obtained by substituting equations (42a), (42b), and (42c) into equations (40a), (40b), and (40c). This results in a matrix equation of the following form:

$$\left\{[K] + [Q]\right\}[Z] = 0 \tag{43}$$

where

$$[K] = \begin{bmatrix} (1 + T)n^2 + P + S & n(T + S + 1) + nP & R(P + S) + Rn^2 \\ n(T + S + 1) + nP & T + 1 + n^2(P + S) & Rn(P + S) + Rn \\ P + S + n^2 & n(P + S) + n & R(P + S) + Rn^2 \end{bmatrix} \tag{44a}$$

$$[Z] = \begin{bmatrix} \bar{u}_1 \\ \bar{u}_2 \\ \bar{\omega}_3 \end{bmatrix} \tag{44b}$$

and where $[Q]$ takes one of the following forms:

$$[Q]_a = \bar{q} \begin{bmatrix} -(1 + c) & -n(1 + c) & 0 \\ -nc & -n^2(1 + c) + 1 & -nRc \\ 0 & 0 & -Rc \end{bmatrix} \tag{44c}$$

$$[Q]_b = \bar{q} \begin{bmatrix} -c & -n(1 + c) & -Rc \\ -nc & -n^2(1 + c) + 1 & -nRc \\ -c & 0 & -Rc \end{bmatrix} \tag{44d}$$

$$[Q]_c = \bar{q} \begin{bmatrix} -c & -nc & -Rc \\ -nc & -n^2(1 + c) + 1 & -nRc \\ -c & -nc & -Rc \end{bmatrix} \tag{44e}$$

The critical load for each of the three loading conditions is obtained by setting the determinant

$$\left|[K] + [Q]\right| = 0 \tag{45}$$

A first-order approximation to these critical loads can be obtained by expanding the determinant and keeping only the terms which are linear in $\bar{q}$ and c. (The results of this procedure were found to give answers within 5 percent of those obtained from the exact solution for $c \leq 0.1$). The lowest buckling mode is for $n = 2$ so that the result of this expansion is:

For constant-direction loading:

$$\bar{q}_{cr} = \frac{4}{1 + \frac{2}{3}c + \frac{4(1+c)}{S+P} + \frac{1+2c}{T}} \tag{46}$$

For radial loading:

$$\bar{q}_{cr} = \frac{4.5}{1 + \frac{3}{2}c + \frac{4 + 4.5c}{S+P}} \tag{47}$$

For hydrostatic loading:

$$\bar{q}_{cr} = \frac{3}{1 + \frac{4 + 3c}{S+P}} \tag{48}$$

Out-of-plane buckling.- The out-of-plane buckling solutions for the two loading conditions are obtained by substituting equations (42d), (42e), and (42f) into equations (40d), (40e), and (40f). This results in equations of the form

$$\left\{[\bar{K}] + [\bar{Q}]\right\}[\bar{Z}] = 0 \tag{49}$$

where

$$[\bar{K}] = \begin{bmatrix} n^2\left(S + P + \frac{3}{8}\Gamma\right) & nR\left(S + P - \frac{\Gamma}{8}\right) & -\frac{\Gamma R n^2}{2} \\ n\left(S + P - \frac{\Gamma}{8}\right) & R\left(n^2 + S + P + \frac{3\Gamma}{8}\right) & Rn\left(\frac{\Gamma}{2} + 1\right) \\ -\frac{\Gamma n^2}{2} & Rn\left(\frac{\Gamma}{2} + 1\right) & R(\Gamma n^2 + 1) \end{bmatrix} \tag{50a}$$

$$\left[\bar{Z}\right] = \begin{bmatrix} \bar{u}_3 \\ \bar{\omega}_2 \\ \bar{\omega}_1 \end{bmatrix} \tag{50b}$$

and where $\left[\bar{Q}\right]$ takes on one of the following forms:

$$\left[\bar{Q}\right]_a = \bar{q}\begin{bmatrix} -n^2(1+c) & 0 & 0 \\ 0 & 0 & 0 \\ 0 & 0 & -Rc \end{bmatrix} \tag{50c}$$

$$\left[\bar{Q}\right]_b = \bar{q}\begin{bmatrix} -n^2(1+c)+1 & 0 & Rc \\ 0 & 0 & 0 \\ c & 0 & -Rc \end{bmatrix} \tag{50d}$$

Setting

$$\left|\left[\bar{K}\right] + \left[\bar{Q}\right]\right| = 0 \tag{51}$$

leads to the buckling loads.

As before, a first-order approximation to these critical loads can be obtained by expanding the determinant and keeping only the terms which are linear in $\bar{q}$ and c. Also, the lowest buckling mode is for $n = 2$ so that the result of this expansion is

For constant-direction loading:

$$\bar{q}_{cr} = \frac{9 + \frac{1.125\Gamma}{P+S}}{4 + 5c + \frac{1+5c}{\Gamma} + \frac{12.375 + 13.875c}{P+S} + \frac{\Gamma}{P+S}(0.5 + 0.625c)} \tag{52}$$

For radial loading:

$$\bar{q}_{cr} = \frac{12 + \frac{1.5\Gamma}{P+S}}{4 + 4c + \frac{1+4c}{\Gamma} + \frac{12.375 + 13.5c}{P+S} + \frac{\Gamma}{P+S}(0.5 + 0.5c)} \tag{53}$$

Note that in equations (46), (47), (48), (52), and (53), the internal-pressure parameter P and shear-stiffness parameter S always appear in combination $(P + S)$ so that the shear stiffness is augmented by the internal pressure contribution. Thus $P + S$ can be considered as an effective transverse shear stiffness.

DISCUSSION OF RESULTS

The results of this analysis can be compared with results obtained by other investigators if the shear and extensional stiffnesses are assumed to be infinitely large and the radius ratio c is neglected. For these cases equations (46), (47), (48), (52), and (53) become, respectively:

$$\bar{q}_{cr} = 4 \qquad \text{(In-plane buckling, constant-direction loading)} \qquad (54a)$$

$$\bar{q}_{cr} = 4.5 \qquad \text{(In-plane buckling, radial loading)} \qquad (54b)$$

$$\bar{q}_{cr} = 3 \qquad \text{(In-plane buckling, hydrostatic loading)} \qquad (54c)$$

$$\bar{q}_{cr} = \frac{9}{4 + \frac{1}{\Gamma}} \qquad \text{(Out-of-plane buckling, constant-direction loading)} \qquad (54d)$$

$$\bar{q}_{cr} = \frac{12}{4 + \frac{1}{\Gamma}} \qquad \text{(Out-of-plane buckling, radial loading)} \qquad (54e)$$

Equation (54a) agrees with results given by Ratzersdorfer (ref. 1) and equations (54d) and (54e) agree with Timoshenko (ref. 3). Equations (54b) and (54c) agree with results given by Boresi (ref. 2). Boresi also included the effect of ring thickness, which will be discussed later.

The effects of finite shear stiffness with appropriate contribution of internal pressure and radius ratio c on the buckling load can be seen by referring to figures 8 and 9. The results shown in these figures were obtained from the approximate equations (46), (47), (48), (52), and (53). However, they are quite accurate for the ranges of ring parameters $\left(c,\ 1/T,\ \Gamma,\ 1/(S + P)\right)$ considered here.

In figure 8 the in-plane buckling load parameter $\bar{q}_{cr}$ (obtained from eqs. (46), (47), and (48)) is plotted against the shear-stiffness parameter $1/(S + P)$ for $c = 0$ and 0.1 with the extensional stiffness parameter $1/T$ equal to zero. It can be seen that the critical load is influenced significantly by changes in the direction of loading during deformation. It is also seen that the critical load is influenced by c and that this influence is likewise dependent on the direction of loading. For example, as c increases $\bar{q}$ is

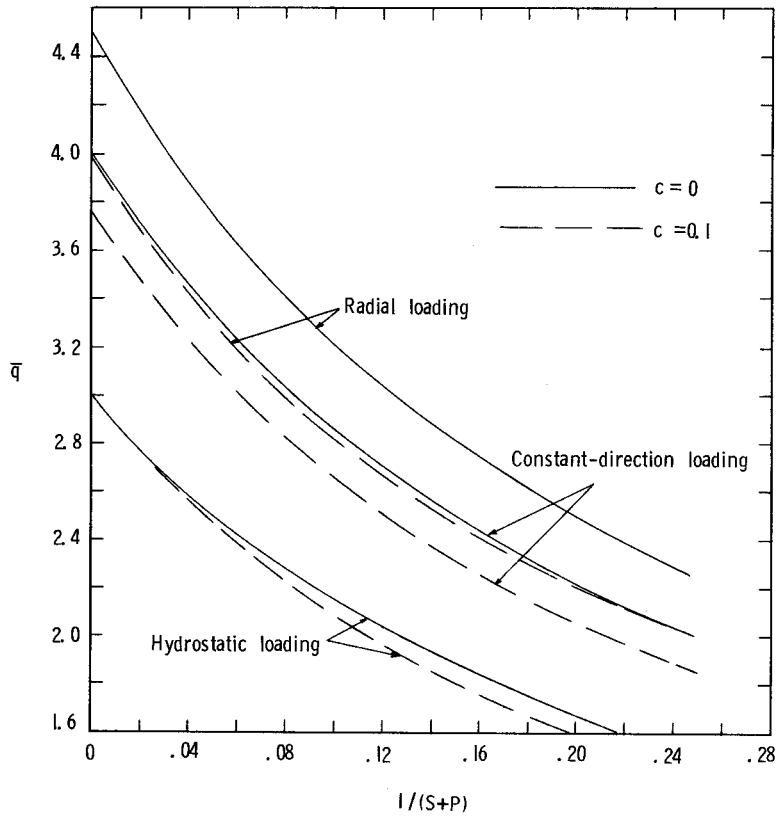

Figure 8.- Variation of in-plane critical load parameter with effective shear-stiffness parameter.

decreased. The influence of ring depth on the buckling load parameter shows the same trends that were obtained by Boresi (ref. 2) for the radial and hydrostatic loading conditions of a ring of rectangular cross section. However, there appears to be no literature available for the constant-direction loading with the effects of ring depth included. Calculations were also carried out for finite but realistic values of $1/T$ in the range $0 \leqq \frac{1}{T} \leqq 0.01$ for the constant-direction loading case (eq. (46)). Throughout this range, the values of $\bar{q}_{cr}$ changed so slightly that the differences could not be plotted in figure 8. Thus, ring extension has little influence on in-plane buckling in the $n = 2$ mode. This would not be the case, however, if external constraints forced buckling in a higher mode.

Note that in all cases, the critical load parameter markedly decreases with an increase in the shear stiffness parameter $1/S + P$. Furthermore, since the pressure parameter P always appears with the shear parameter, the internal pressure will have no effect if the shear stiffness of the membrane wall is large ($S = \infty$).

In figure 9, the out-of-plane buckling load parameter $\bar{q}_{cr}$ (obtained from eqs. (52) and (53)) is plotted against shear stiffness parameter $1/S + P$ for $c = 0$ and 0.1 with twisting stiffness $\Gamma = 1.0$. It can be seen that, as in the in-plane buckling case, the

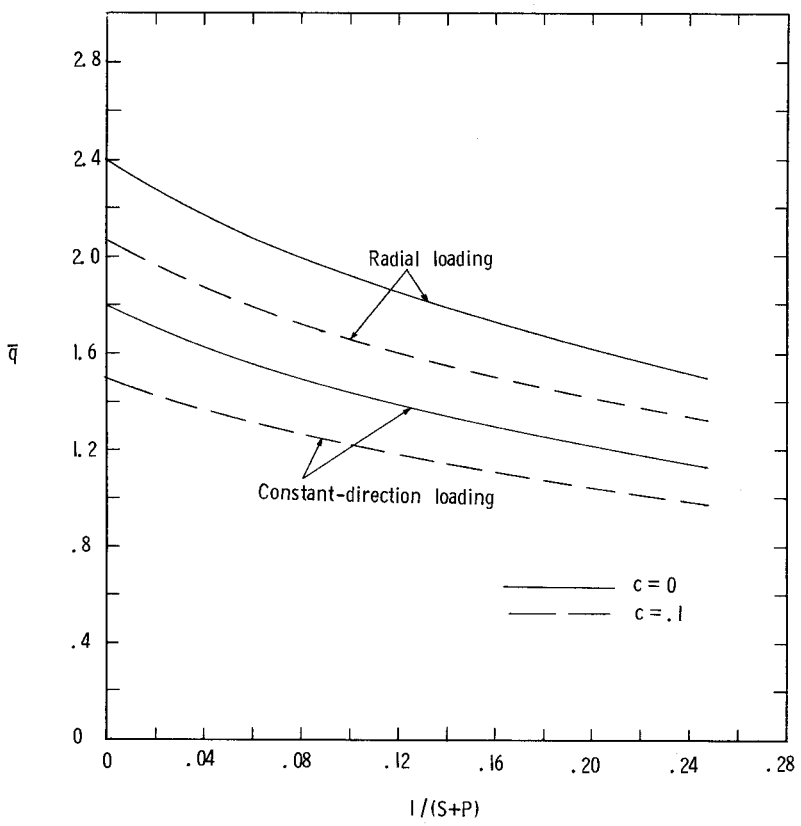

Figure 9.- Variation of out-of-plane critical load parameter with effective shear-stiffness parameter for $\Gamma = 1$.

direction of loading during deformation, as well as the value of c, significantly affects the magnitude of the buckling load. In all cases the buckling load parameter decreases with an increase in $1/S + P$. Also, the out-of-plane buckling loads are lower than the in-plane buckling loads for the same external loading conditions and geometrical properties. Note in equations (54d) and (54e) the potentially large effect of the parameter Γ on out-of-plane buckling. Evidently, if $\Gamma = 1$, drastic reductions in the buckling load occur. Such low values may be possible for deployable toroidal rings constructed from single layers of organic or metallic fabric (see, for example, ref. 6).

It is interesting to note that the in-plane and out-of-plane buckling modes are uncoupled. This is true because the product of inertia for the toroidal ring is zero. A consequence of this uncoupling is that the twisting stiffness Γ does not affect in-plane buckling and the extensional stiffness T does not influence out-of-plane buckling.

CONCLUDING REMARKS

A theoretical investigation of the buckling of a pressurized toroidal ring under a uniformly distributed line load has been carried out, with finite shear stiffness,

extensional stiffness, and the appropriate contributions from the internal pressure taken into account. The equations governing both in-plane and out-of-plane buckling behavior of the ring for three directions of loading have been derived and solved, and simple buckling formulas are given.

The major results of the investigation are:

1. The magnitude of the buckling load is very sensitive to the direction of loading during the buckling deformations, and also to the ratio of cross-sectional radius to radius of the ring.

2. Out-of-plane buckling loads are lower than the in-plane buckling loads for the same external loading conditions.

3. Shear stiffness of the ring wall material and internal pressure both contribute to the effective transverse shear stiffness of the ring, which strongly influences buckling strength.

4. The effect of extensional stiffness on the in-plane buckling load is negligible. However, twisting may strongly influence the buckling loads. Out-of-plane buckling behavior does not couple with in-plane buckling behavior.

Langley Research Center,
National Aeronautics and Space Administration,
Langley Station, Hampton, Va., March 3, 1967,
124-08-06-21-23.

REFERENCES

1. Ratzersdorfer, Julius: The Buckling of a Thin Circular Arch. Engineering, Vol. 150, Oct. 11, 1940, pp. 284-285.

2. Boresi, A. P.: A Refinement of the Theory of Buckling of Rings Under Uniform Pressure. J. Appl. Mech., vol. 22, no. 1, Mar. 1955, pp. 95-102.

3. Timoshenko, S.: Theory of Elastic Stability. McGraw-Hill Book Co., Inc., 1936, pp. 285-286.

4. Fichter, W. B.: A Theory for Inflated Thin-Wall Cylindrical Beams. NASA TN D-3466, 1966.

5. Novozhilov, V. V.: Foundations of the Nonlinear Theory of Elasticity. Graylock Press, 1953.

6. Leonard, Robert W.: On the Shear Stiffness of Fabrics. J. Aerospace Sci. (Readers' Forum), vol. 29, no. 3, Mar. 1962, pp. 349-350.

NASA-Langley, 1967 —— 32 L-5003